Computer Simulation of Variable-Parameter Kinetic Experiments

Giuseppe Alibrandi,* Santi D'Aliberti, and Rolando Pedicini

Dipartimento di Chimica Inorganica, Chimica Analitica e Chimica Fisica, Università di Messina , Salita Sperone 31, Vill. S. Agata, 98166 Messina, Italy, Alibrandi@chem.unime.it

Received November 27, 2000. Accepted March 1, 2001

Abstract: Computer simulations of variable-parameter kinetic experiments have been performed using a program requiring as input a function linking the parameter to the time and a function linking the rate constant to the parameter.

Introduction

Kinetics is the traditional means of studying reaction mechanisms. The usual method is to determine the first- or pseudo-first-order rate constants for the reaction being studied for different experimental conditions; then correlate them with a parameter (e.g., temperature, T; pressure, P; concentration, C_i) to obtain the information ($\Delta H^{\ddagger}$, $\Delta S^{\ddagger}$, $\Delta V^{\ddagger}$, the empirical rate law, etc.) required to propose a reaction scheme [1–3]. Recently, some efforts have been made to obtain in a single kinetic experiment the dependence of the rate constant on a given parameter [4–13]. This is possible simply by varying the value of the parameter in a known way while the experiment is carried out. The general equation for variable-parameter kinetics (VPaK) [7] is

$$v = -\frac{dC}{dt} = k_{\text{obs}}\left[Par_i(t)\right]C \qquad (1)$$

where C is the concentration of the reacting species and v is the rate, which depends on the contribution of two varying terms: $C = C(t)$ and $k_{\text{obs}} = k_{\text{obs}}[Par_i(t)]$. The parameter $Par_i(t)$ varies with time. The integral form, shown in eq 2, describes the trend in the concentration of the reacting species during the process.

$$C = C_0 \exp(-\int_0^t k_{\text{obs}}\left[Par_i(t)\right]dt) \qquad (2)$$

By processing the experimental data, the ratio $-(dC/dt)/C$ gives the $k_{\text{obs}}(Par_i)$ profile (eq 1), that is, the entire dependence of k_{obs} on the parameter. Furthermore, if the mathematical form of the function $k_{\text{obs}}[Par_i(t)]$ is known, a direct best fit to either eq 1 or eq 2 gives the optimized values of the terms controlling the dependence of k_{obs} on that parameter.

For the performance of these kinetic experiments to be useful, it is necessary to be able to easily (1) produce variable-parameter conditions, (2) automatically collect concentration-versus-time data, and (3) quickly process the stored data.

In the past, variable-temperature kinetics has been treated as nonisothermal kinetics [4–6]. Nevertheless, its application in the study of reaction mechanisms has been limited by the availability of equipment. Recently variable-concentration kinetics [7, 13] and variable-temperature kinetics [8, 10, 11] were proposed theoretically as particular cases of general variable-parameter kinetics. Experimentally, modern instruments are used to control the parameters, and modern computers are used to collect and process the kinetic data. This new approach, now possible because of advances in technology, allows us to consider VPaK experiments as routine.

The aim of this paper is to show how the kinetic profile of such reactions can be obtained by computer simulation. This is valuable when the instrumentation needed for the experiments is not available. It is important to have an overview of the subject and to explore the potential of this new method of collecting kinetic data.

Computational Section

Any software (Mathematica, Mathlab, etc.) capable of processing and plotting functions and containing algorithms for numerical integration can be used for these types of simulations [14]. The examples given in this paper were obtained using the MicroMath SCIENTIST software program because of its easy-to-use interface, which greatly facilitates model entry and manipulation. Only a few lines of programming are necessary to define a model that is based on eq 1 written in the form

$Par_i(t)$	Function linking the parameter to the time
$k_{\text{obs}}(Par_i)$	Function linking the rate constant to the parameter
$C' = -k_{\text{obs}}*C$	First-order differential equation

Different profiles can be obtained by varying the first two functions by changing (1) the parameter, (2) the way the parameter changes with time, and/or (3) the way the parameter influences the rate constant.

Table 1 shows a list of the functions used in this paper. They will be illustrated later. For variable-temperature kinetics (VTK; $Par_i = T$), for example, eq 1 takes the form shown in eq 3

$$-\frac{dC}{dt} = k_{\text{obs}}\left[T(t)\right]C \qquad (3)$$

Table 1. List of Parameters (Par_i), Modulating Functions ($Par_i(T)$), and Dependence Functions ($k_{obs}(Par_i)$) Used for Simulation of Variable-Parameter Kinetic Experiments

Par_i	$Par_i(t)$	$k_{obs}(Par_i)$	
T	$T = T_0$	$k_{obs} = \frac{kT}{h}\exp\left(\frac{\Delta S^{\ddagger}}{R}\right)\exp\left(-\frac{\Delta H^{\ddagger}}{RT}\right)$	(I)
T	$T = T_0 + \alpha t$	$k_{obs} = \frac{kT}{h}\exp\left(\frac{\Delta S^{\ddagger}}{R}\right)\exp\left(-\frac{\Delta H^{\ddagger}}{RT}\right)$	(II)
T	$T = T_0 + \alpha t + \beta t^2$	$k_{obs} = \frac{kT}{h}\exp\left(\frac{\Delta S^{\ddagger}}{R}\right)\exp\left(-\frac{\Delta H^{\ddagger}}{RT}\right)$	(III)
T	$T=T_{\mathrm{m}}+\frac{\mathrm{A}}{2}\sin\left(\frac{2\pi t}{L}+\frac{3\pi}{2}\right)$	$k_{obs} = \frac{kT}{h}\exp\left(\frac{\Delta S^{\ddagger}}{R}\right)\exp\left(-\frac{\Delta H^{\ddagger}}{RT}\right)$	(IV)
T	$T=T_{\mathrm{m}}+\frac{\mathrm{A}}{2}\sin\left(\frac{2\pi t}{L}+\frac{3\pi}{2}\right)+\alpha\iota$	$k_{obs} = \frac{kT}{h}\exp\left(\frac{\Delta S^{\ddagger}}{R}\right)\exp\left(-\frac{\Delta H^{\ddagger}}{RT}\right)$	(V)
P	$P = P_0 + \alpha t$	$k_{obs} = k_0 \exp\left(-\frac{\Delta V^{\ddagger} P}{RT}\right)$	(VI)
P	$P = P_{\mathrm{f}}\left[1-\exp\left(-k_d t\right)\right]$	$k_{obs} = k_0 \exp\left(-\frac{\Delta V^{\ddagger} P}{RT}\right)$	(VII)
P	$P=P_{\mathrm{m}}+\frac{\mathrm{A}}{2}\sin\left(\frac{2\pi t}{L}+\frac{3\pi}{2}\right)$	$k_{obs} = k_0 \exp\left(-\frac{\Delta V^{\ddagger} P}{RT}\right)$	(VIII)
C_{Y}	$[Y] = \alpha t$	$k_{obs} = k_{\mathrm{S}} + k_{\mathrm{Y}}[Y]$	(IX)
C_{Y}	$[Y] = \frac{10^{-6}}{\left(10^{-3} - 10^{-6} t\right) k_{\mathrm{Y}}}$	$k_{obs} = k_{\mathrm{Y}}[Y]$	(X)
C_{Y}	$[Y] = [Y]_0 \exp\left(-k_d t\right)$	$k_{obs} = \frac{k_{\mathrm{D}} K_{\mathrm{e}} + k_1 [Y]}{K_{\mathrm{e}} + [Y]}$	(XI)
C_{Y}	$[Y] = [Y]_0 + \alpha t$	$k_{obs} = \frac{k_1 [Y]}{k_2 [Z] + [Y]}$	(XII)
C_{Z}	$[Z] = [Z]_0 \exp\left(-k_d t\right)$	$k_{obs} = \frac{k_1 [Y]}{k_2 [Z] + [Y]}$	(XIII)
$C_{\mathrm{Y}}, C_{\mathrm{Z}}$	$[Y] = [Y]_{\mathrm{m}} + \frac{\mathrm{A}}{2}\sin\left(\frac{2\pi t}{L}+\frac{3\pi}{2}\right)$ $[Z] = [Z]_{\mathrm{m}} + \frac{\mathrm{A}}{2}\sin\left(\frac{2\pi t}{L}+\frac{3\pi}{2}\right)$	$k_{obs} = [Y]\frac{k_{\mathrm{Y}} + k_{\mathrm{Z}} K_{\mathrm{e}} [Z]}{1 + K_{\mathrm{e}} [Z]}$	(XIV)
T, C_{Y}	$T=T_{\mathrm{m}}+\frac{\mathrm{A}}{2}\sin\left(\frac{2\pi t}{L}+\frac{3\pi}{2}\right)$ $[Y] = \alpha t$	$k_{\mathrm{Y}} = \frac{kT}{h}\exp\left(\frac{\Delta S^{\ddagger}}{R}\right)\exp\left(-\frac{\Delta H^{\ddagger}}{RT}\right)$ $k_{obs} = k_{\mathrm{Y}}[Y]$	(XV)

where the function linking the rate constant to the temperature, $k_{\mathrm{obs}}(T)$, can be the Eyring equation (eq 4)

$$-\frac{dC}{dt} = \frac{k_B T(t)}{h}\exp\left(\frac{\Delta S^{\ddagger}}{R}\right)\exp\left(-\frac{\Delta H^{\ddagger}}{RT(t)}\right)C \qquad (4)$$

where $\Delta H^{\ddagger}$ and $\Delta S^{\ddagger}$ are the enthalpy and the entropy of activation. Selecting a series of functions, $T(t)$, it is possible to obtain the relative kinetic profiles. For the simple case of a linear temperature increase, the program will be

$$T = T_0 + \alpha * t$$

$$k_{\mathrm{obs}} = \left(k_B * T / h\right) * \exp\left(\Delta S^{\ddagger} / R\right) * \exp\left(-\Delta H^{\ddagger} / \left(R * T\right)\right)$$

$$C' = k_{\mathrm{obs}} * C$$

Both modulating functions and dependence functions contain mathematical terms (α, β, A, etc.) that depend on the

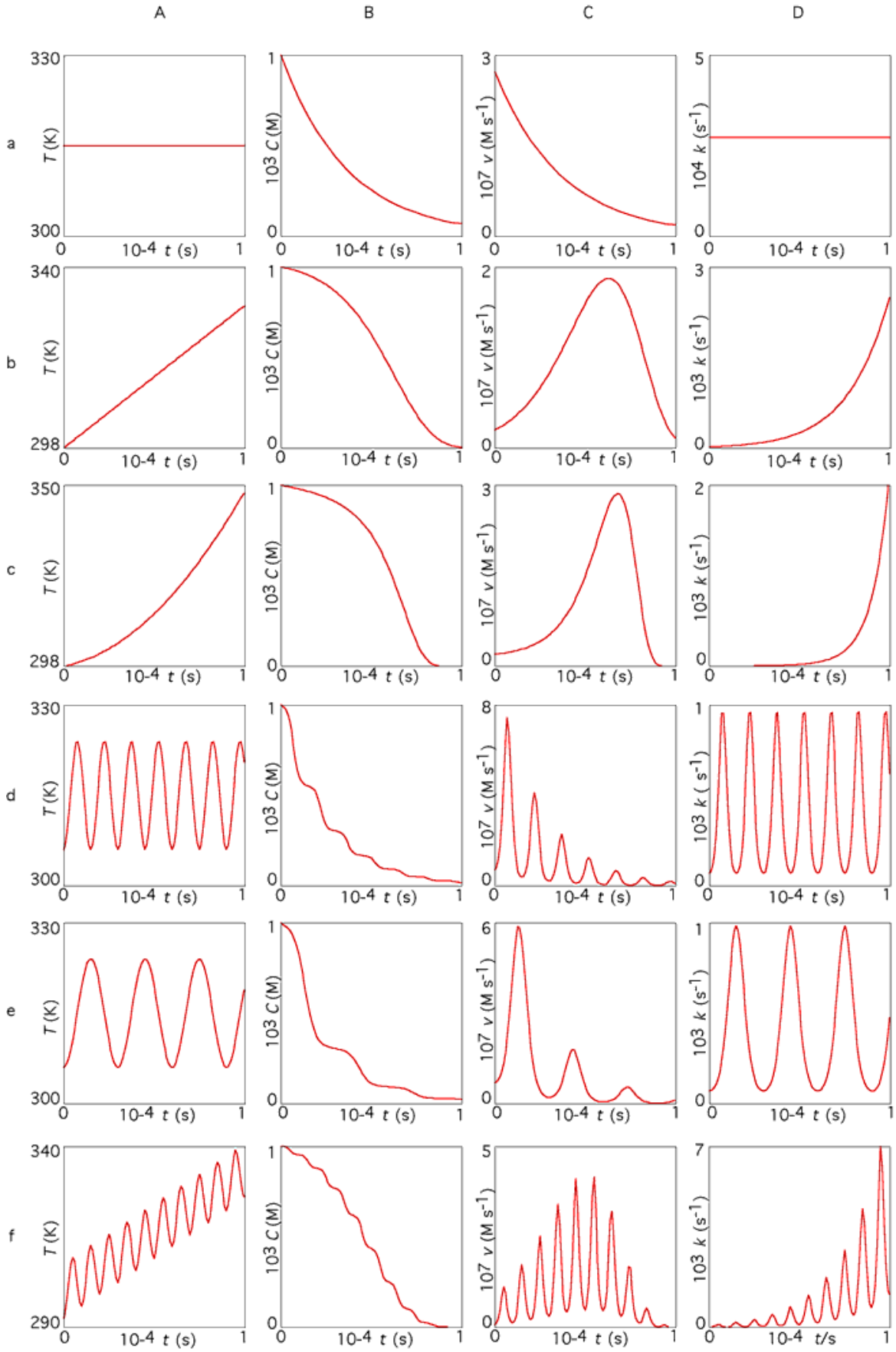

Figure 1. Trends in the temperature (column A), concentration (column B), reaction rate (column C), and rate constant (column D) as obtained by computer simulation of variable-temperature kinetic experiments for a reaction having $\Delta S^{\ddagger} = 61$ J K^{-1} mol^{-1}, $\Delta H^{\ddagger} = 118$ kJ mol^{-1} and $C_0 = 1 \times 10^{-3}$ M. Rows refer to temperature functions that are (a) constant, (b) linear, (c) parabolic, (d, e) sinusoidal, and (f) sinusoidal + linear.

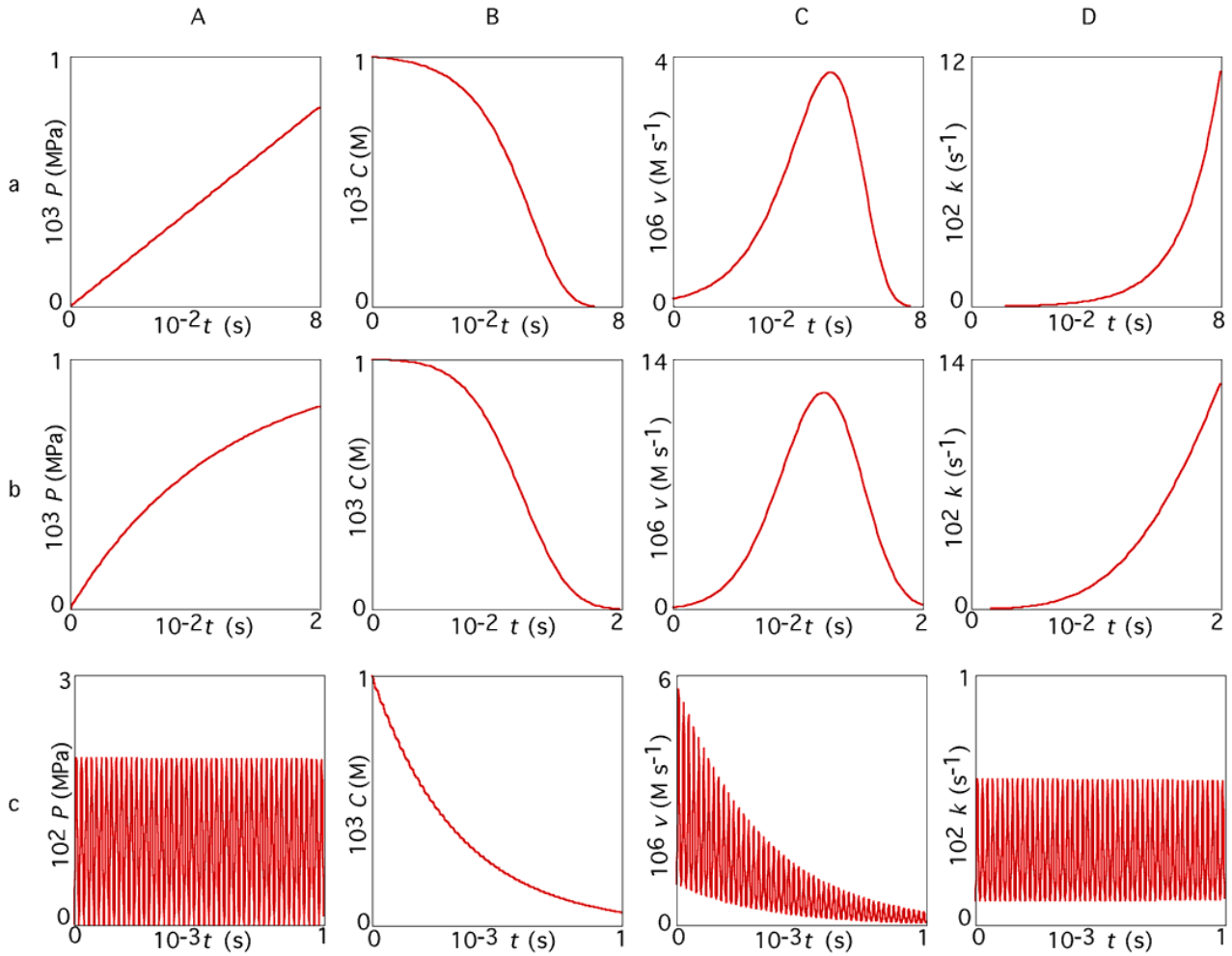

Figure 2. Trends in the pressure (column A), concentration (column B), reaction rate (column C), and rate constant (column D) as obtained by computer simulation of variable-pressure kinetic experiments for a reaction having $\Delta V^{\ddagger} = -20$ cm^3 mol^{-1} and $C_0 = 1 \times 10^{-3}$ M. Rows refer to pressure functions that are (a) linear, (b) exponential, and (c) sinusoidal.

simulation. They are constants and their numerical values have to be assigned for each case, as shown below.

Results and Discussion

Figure 1 shows some kinetic profiles obtained in this way (column B) beside the relative functions, $T(t)$, (column A) used to generate them. The decreasing functions, $C(t)$, are modulated by the functions $T(t)$, and the reaction rates (column C) at each point are given by the product of the two terms $k_{obs}[T(t)]$ (column D) and $C(t)$. All simulations were made using the activation parameter values, $\Delta S^{\ddagger}$ and $\Delta H^{\ddagger}$, of 61 J K^{-1} mol^{-1} and 118 kJ mol^{-1}, respectively, and an initial concentration, C_0, of 1×10^{-3} M [15].

Row a of Figure 1 refers to a traditional constant-temperature kinetic experiment (function I in Table 1) with $T_0 = 315$ K. The concentration and the reaction rate decrease exponentially with time while the rate constant remains *constant*. In row b of Figure 1 (function II), the temperature increases linearly ($T_0 = 298$ K and $\alpha = 3.3 \times 10^{-3}$ K s^{-1}) so that the reaction is at first accelerated because of the increase of k_{obs} and then decelerated when the increase of k is overcome by the decrease in C. For row c of Figure 1 (functions III), the increase is parabolic ($T_0 = 298$ K, $\alpha = 1.0 \times 10^{-3}$ K s^{-1} and $\beta = 4.0 \times 10^{-7}$ K s^{-2}) so that the acceleration is greater. Rows d and e of Figure 1 (function IV) show the effect of sinusoidal variations of T around a temperature, T_m, of 315 K with amplitude, A, and period, L, of 18 K and 1500 s (row d) and 18 K and 3000 s (row e), respectively. The kinetic profiles are composed of more sigmoidal pieces, the rate constants vary sinusoidally, and the reaction rates have the profile of damped oscillations. In row f of Figure 1 (function V), $T(t)$ is a combination of two functions, one sinusoidal and one linear ($T_m = 300$ K, $A = 15$ K, $L = 1000$ s, $\alpha = 3.3 \times 10^{-3}$ K s^{-1}). The kinetic profile has the shape of a sigmoid composed of more sigmoids. The rate constant increases by an amplified oscillation while the reaction rate varies by an amplified oscillation in the first part of the reaction and by a damped oscillation in the second part.

For variable-pressure kinetics (VPK), $P(t)$ functions must be entered in the program together with the function $k_{obs}(Par_i) = k_{obs}(P)$ that has the form of eq 5

$$k_{obs} = k_0 \exp\left(-\frac{\Delta V^{\ddagger} P}{RT}\right) \qquad (5)$$

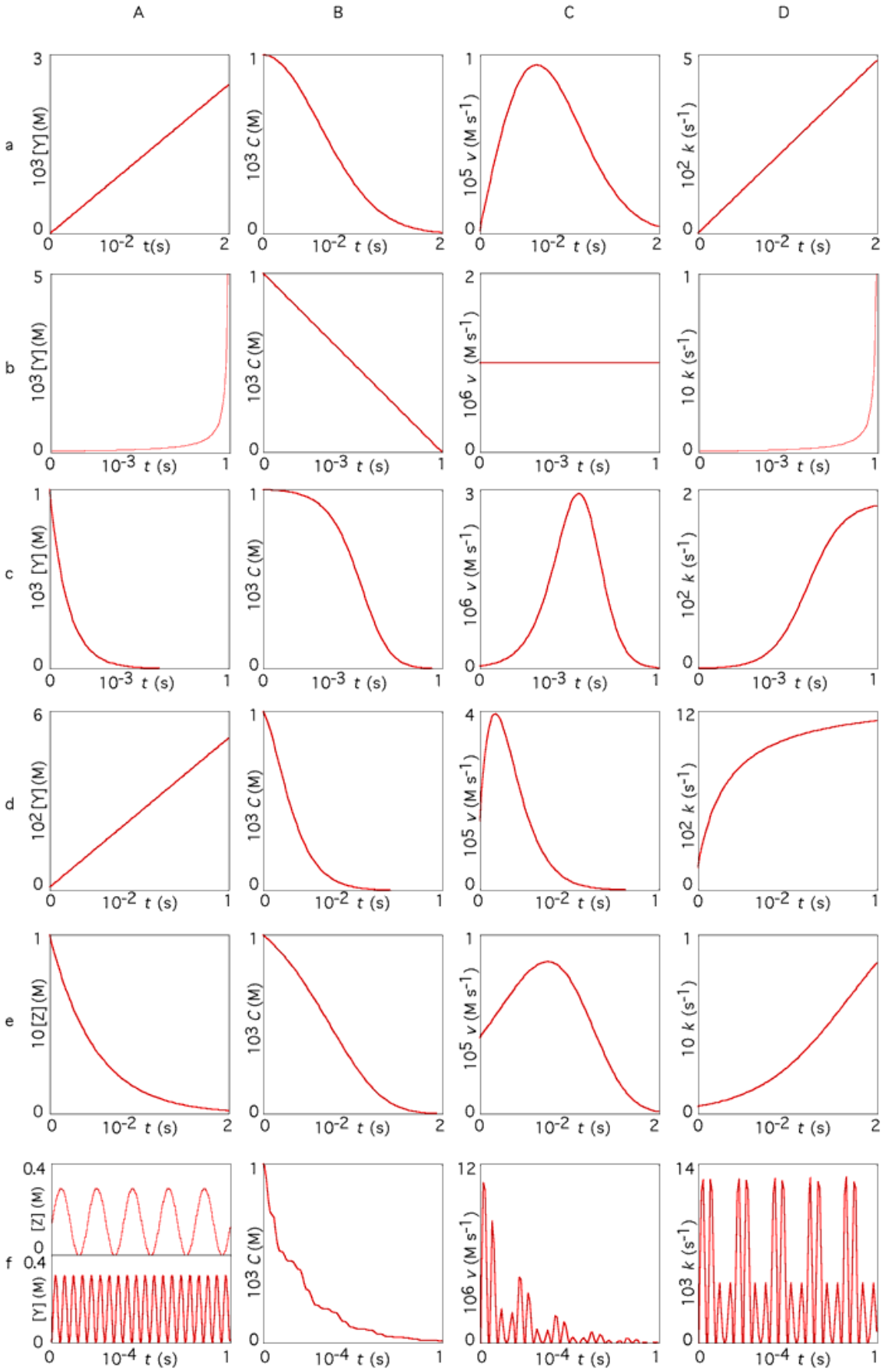

Figure 3. Trends in the concentration of reactants present in the rate law (column A), concentration (column B), reaction rate (column C), and rate constant (column D) as obtained by computer simulation of variable-concentration kinetic experiments for reactions having different rate laws and $C_0 = 1 \times 10^3$ M. Rows refer to concentration functions that are (a, d) linear, (b) hyperbolic, (c, e) exponential, (f) sinusoidal.

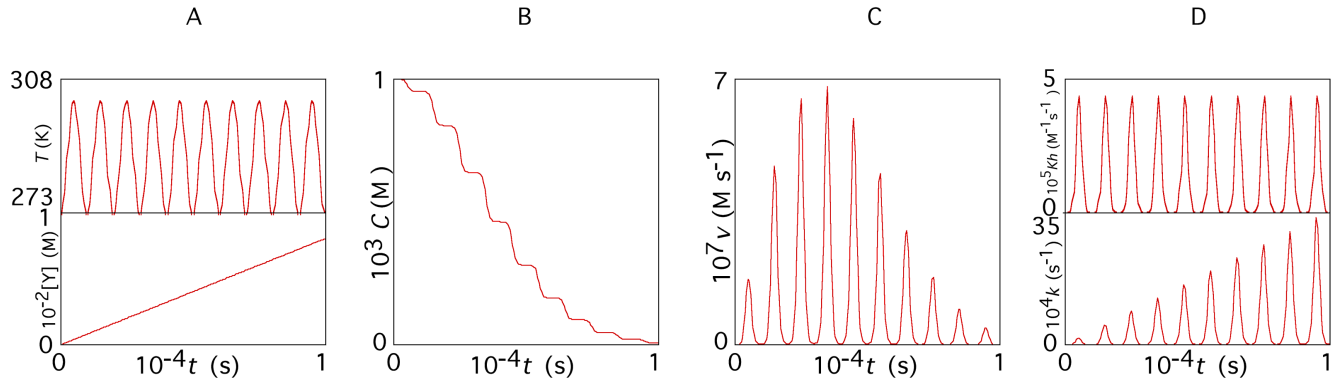

Figure 4. Trends in the concentration of reactants present in the rate law and of temperature (column A), concentration (column B), reaction rate (column C), and rate constant (column D) as obtained by computer simulation of variable-concentration/temperature kinetic experiments for a reaction having a rate law of $k_{obs} = k_Y[Y]$, $\Delta S^{\ddagger} = 61$ J K^{-1} mol^{-1}, $\Delta H^{\ddagger} = 118$ kJ mol^{-1} and $C_0 = 1 \times 10^{-3}$ M. Temperature varies linearly and concentration sinusoidally.

where $\Delta V^{\ddagger}$ is the activation volume. In Figure 2 there are three examples of VPK simulations obtained for a reaction having $\Delta V^{\ddagger} = -20$ cm^3 mol^{-1} [2]. The first simulation, row a of Figure 2 (function VI), refers to a linear pressure increase between 0.1 and 800 MPa ($P_0 = 0.1$ MPa, $\alpha = 1$ MPa s^{-1}; $k_0 = 1 \times 10^{-4}$ s^{-1}). It has a sigmoidal profile very similar to that obtained for VTK simulation with linear $T(t)$. The second simulation, row b of Figure 2 (function VII), which has an exponential modulating function ($P_f = 1000$ MPa, $k_d = 1 \times 10^{-2}$ s^{-1}; $k_0 = 1 \times 10^{-4}$ s^{-1}), has the same shape but is less accelerated at the end. The third simulation, row c of Figure 2 (function VIII), is modulated by a sinusoidal function with a relatively high frequency (P_m = 100.1 MPa, $A = 200$ MPa, $L = 20$ s; $k_0 = 1 \times 10^{-3}$ s^{-1}). It shows a waving exponential decrease in C and a damped decreasing wave in the rate.

For variable-concentration kinetics (VCK), several equations for $k_{obs}(Par_i) = k_{obs}(C_i)$ can be used that depend on the rate law linking the observed rate constant to the concentrations of the species present in the reaction environment and influencing the rate determining step. Modulation is ensured by functions $Par_i(t) = C_i(t)$ containing kinetic constants for elementary steps and, sometimes, equilibrium constants. Figure 3 shows some examples. Row a of Figure 3 (function IX) was generated by a rate law of the type $k_{obs} = k_S + k_Y[Y]$ (Y is a nucleophile in a nucleophilic substitution in a square planar complex.) [16] and a linear concentration increase, $[Y] = \alpha t$ ($k_S = 1.87 \times 10^{-4}$ s^{-1}, $k_Y = 19.3$ M^{-1}s^{-1}, $\alpha = 1.25 \times 10^{-5}$ M s^{-1}). Here the acceleration of the rate in the first part of the reaction due to the increase in k_{obs} caused by increasing concentration of reactant Y generates a sigmoidal shape. The rate reaches a maximum and then goes back to zero while the concentration of the reacting species goes to zero. In row b of Figure 3 (function X), for a rate law $k_{obs} = k_Y[Y]$ (with Y a nucleophile, catalyst, etc.), the concentration of the species is forced to decrease linearly by using a modulating function $[Y] = 10^{-6}/[(10^{-3} - 10^{-6}t)k_Y]$ where $k_Y = 19.3$ M^{-1} s^{-1}. The reaction rate is always constant because the increase in the rate constant exactly compensates for the decrease in C. Row c of Figure 3 (function XI) refers to a reaction whose rate is inhibited by a reactant Y ($k_D = 1.86 \times 10^{-4}$ s^{-1}, $k_I = 0.01 \times 10^{-4}$ M^{-1} s^{-1}, $K_e = 2.14 \times 10^{-6}$) [15]. In this case there is an exponential decrease in the concentration of Y that causes the acceleration in the first part of the reaction and the sigmoidal shape ($[Y]_0 = 1 \times 10^{-3}$ M, $k_d = 1 \times 10^{-2}$ s^{-1}). Row d and e of Figure 3 (functions XII and XIII) were generated by the same rate law where k_{obs} depends on the concentration of two species: Y and Z ($k_1 = 0.13$ s^{-1}, $k_2 = 1 \times 10^{-6}$) [17]. For the former, the acceleration is caused by an increase in [Y] ([Z] = 5×10^{-3} M, $[Y]_0 = 1 \times 10^{-3}$ M, $\alpha = 5.0 \times 10^{-4}$ M s^{-1}) while in the latter it is due to a decrease in the concentration of the inhibitor Z ([Y] = 5×10^{-3} M, $[Z]_0 = 0.1$ M, $k_d = 2 \times 10^{-2}$ s^{-1}).

Finally, two more simulations are proposed where the values of more parameters are changed with time. The first (row f of Figure 3, function XIV) refers to a reaction conditioned by two reactants ($k_Y = 0.38 \times 10^{-3}$ M^{-1} s^{-1}, $k_Z = 1.28 \times 10^{-2}$ M^{-1} s^{-1}, K_e = 1.97 M^{-1}) [18]. The simulation is obtained by varying sinusoidally the concentration of both reactants, [Y] ($[Y]_m$ = 0.15 M, $A = 0.3$ M, $L = 500$ s) and [Z] ($[Z]_m = 0.15$ M, A = 0.3 M, $L = 2000$ s). The result is a very irregular profile. The second (Figure 4, function XV) refers to a hypothetical reaction with a rate law of $k_{obs} = k_Y[Y]$ and $\Delta S^{\ddagger} = 61$ J K^{-1} mol^{-1} and $\Delta H^{\ddagger} = 118$ kJ mol^{-1}. The simulation is obtained by sinusoidally varying the temperature and linearly varying the concentration of reactant Y ($T_m = 288$ K, $A = 30$ K, $L = 1000$ s, $\alpha = 8.0 \times 10^{-3}$ M s^{-1}). The result is a sigmoid of sigmoids but in this case the functions involved are both the Eyring equation and the rate law.

Conclusions

Computer simulation can be a very powerful tool for exploring variable-parameter kinetics. VPaK profiles, which are often difficult to visualize, can be easily obtained by simply selecting a modulating function and a dependence function. This can be helpful to students interested in kinetics and reaction mechanisms.

References and Notes

1. Moore, J. W.; Pearson, R. G. *Kinetics and Mechanism;* Wiley: New York, 1981.
2. Wilkins, R. G. Kinetics and Mechanism of Reactions of Transition Metal Complexes; VCH: Weinheim, 1991.
3. Loudon, G. M. *J. Chem. Educ.* **1991,** *68,* 973–984.
4. Koch, E. *Nonisothermal Reaction Analysis;* Academic Press: London, 1977.
5. Brown, M. E.; Phillpotts, C. A. R. *J. Chem. Educ.* **1978,** *55,* 556–560.

6. Salvador, F.; Gonzalez. J. L.; Tel, L. M. *J. Chem. Educ.* **1984,** *61,* 921–922.
7. Alibrandi, G. *J. Chem. Soc.*, *Chem. Commun.* **1994,** 2709–2710.
8. Alibrandi, G. *Inorg. Chim. Acta* **1994,** *221,* 31–34.
9. Zhang, S.; Brown, T. L. *Inorg. Chim. Acta* **1995,** *240,* 427–433.
10. Alibrandi, G.; Micali, N.; Trusso, S.; Villari, A. *J. Pharm. Sci.* **1996,** *85,* 1105–1108.
11. Romeo, R.; Alibrandi, G. *Inorg. Chem.* **1997,** *36,* 4822–4830.
12. Hodgson, S. C.; Ngeh, L. N.; Orbell, J. D.; Bigger, S. W. *J. Chem. Educ.* **1998,** *75,* 1150–1153.
13. Alibrandi, G.; Coppolino, S.; Micali, N.; Villari, A. *J. Pharm. Sci.* **2001,** *90,* 270–274.
14. Press, W. H.; Flannery, B. P.; Teukolsky, S. A.; Vetterling, W. T. *Numerical Recipes;* Cambridge University Press: Cambridge, 1986.
15. Romeo, R.; Alibrandi, G.; Monsù Scolaro, L. *Inorg. Chem.* **1993,** *32,* 4688–4694.
16. Tobe, M. L. *Comprehensive Coordination Chemistry;* Wilkinson, G.; Gillard, R. D.; McCleverty, J. A., Eds.; Pergamon, Oxford, 1987, Vol. 1, 281–329.
17. Minniti, D.; Alibrandi, G.; Tobe, M. L.; Romeo, R. *Inorg. Chem.* **1987,** *26,* 3956–3958.
18. Alibrandi, G.; Minniti, D.; Romeo, R.; Uguagliati, P.; Calligaro, L.; Belluco, U.; Crociani, B. *Inorg. Chim. Acta* **1985,** *100,* 107–113.